© 1997 The Chemical Society of Japan Bull. Chem. Soc. Jpn., 70, 1985—1993 (1997) 1985

Synthesis of Nano-Dimensional Iron–Cobalt Spinel Mixed Oxides from Layered-Type Carbonate Hydroxide Precursors

Elly L. Uzunova,* Ivan G. Mitov,† and Dimitar G. Klissurski*

Institute of General and Inorganic Chemistry, Bulgarian Academy of Sciences, Sofia 1113, Bulgaria

†Institute of Catalysis, Sofia 1113, Bulgaria

(Received January 31, 1997)

Pyroaurite-like carbonate hydroxide precursors $Co_{1-x}Fe_x(CO_3)_{x/2}(OH)_2 \cdot nH_2O$, where x varies in the range $0.25 \leq x \leq 0.75$, yield cation deficient mixed oxides with particle dimensions in the nano-scale range. The thermal decomposition and spinel structure formation processes have been studied by thermal analysis and IR spectroscopy, revealing an intermediate of hydroxide oxide type. Mesoporous mixed oxides with cubic spinel structure were synthesised at 300—400 °C with significant contribution of small pores of radii < 200 Å. Oxygen desorption from cobalt ferrite, synthesised at 350 °C, suggests the existence of a high content of extraframework oxygen. The temperature-programmed reduction (TPR) with hydrogen occurs in one stage for all cobalt/iron compositions. The peak maxima shift to higher temperatures and a broadening is observed with increasing the iron content. Partly inverse cation distributions of the spinel ferrites are deduced from the Moessbauer spectra.

A modern trend in the design of inorganic materials is the development of synthetic methods, where each step is performed under mild conditions—e.g. treatment with environmentally friendly reagents in non-extreme, soft chemical and thermal procedures. The thermal decomposition of well-defined crystalline precursors presents the best route for the preparation of a large number of mixed oxides. The choice of an appropriate precursor allows monitoring of the dispersity, particle size and shape, particular oxidation states of the cations, cation distribution, non-stoichiometry, and stabilization of one framework type in cases where different crystallographic forms exist.[1)]

The system Co–Fe–O forms a stable region of isomorphous cobalt–iron substitution with a cubic spinel structure $Co_yFe_{3-y}O_4$ $(0 < y < 3)$ at temperatures below 450 °C. These spinel mixed oxides are metastable and segregate at high temperature to two spinel phases (cobaltite and ferrite) for $1.15 < y < 2.7$, and ferrite+hematite, (α-Fe_2O_3) for $y < 0.9$.[2)] Coprecipitation of different precursor compounds was mostly employed in the synthesis of these compounds, apart from the conventional ceramic synthesis methods by a solid-phase reaction requiring high temperatures. Their applications as magnetic materials, electrode coatings, and catalysts demand high-dispersity, phase purity and homogeneity.[3,4)] Coprecipitated hydroxides are mostly preferred as precursors for the synthesis of substituted magnetites.[5,6)] Extremely low temperatures of thermal decomposition in the synthesis of cobaltite spinels were achieved after coprecipitation in mild conditions by using an organic base.[7)] Preparation of spinel mixed oxides containing iron (γ-Fe_2O_3 and ferrites partly substituted with chromium and aluminum) with a vacancy ordering on octahedral positions was possible, when proceeding from coprecipitated oxalates, by thermal decomposition in oxidizing media.[8)] Coprecipitated calcite-type iron(II)–cobalt(II) carbonates were also used for the synthesis of cation-deficient spinel mixed oxides at low temperature (300 °C), no vacancy ordering being observed in the X-ray patterns.[9)] The iron hydroxide oxides α-FeO(OH) and γ-FeO(OH) illustrate in the best way how a particular precursor compound can direct the synthesis towards the thermodynamically more stable form (hematite, α-Fe_2O_3) or the less stable cubic phase (γ-Fe_2O_3). Introducing a second cation in the lattice certainly has a strong influence on the $\gamma \Rightarrow \alpha$ transition. Compared to pure γ-Fe_2O_3, the cobalt containing spinel phase is more stable.[2,8)]

The structure of layered double hydroxides (LDH) permits broad variation in composition: The divalent/trivalent ratio of metal cations may change considerably, the extra charge being compensated by the anionic layer; a broad number of cations and anionic species may take place in the structure.[11—13)] For pyroaurite analogs, the ratio between divalent and trivalent cations was varied in the ranges $1.6 \leq Mg(II)/Fe(III) \leq 4.5$;[14)]$0.5 \leq [Co(II)+Fe(II)]/Fe(III) \leq 3$;[15)]$0.33 \leq Ni(II)/Fe(III) \leq 3$.[16)] Higher oxidation states like Co(IV) and Fe(IV) were reached electrochemically, while still preserving the layered structure.[17)] The synthesis of nanoscale cobalt ferrite and mixed oxides Co–Fe–O with spinel structure in the range $0.33 < Fe/Co < 3$ from layered cobalt–iron carbonate hydroxide precursors,[15)] obtained by a coprecipitation method, is studied in the present work. The decomposition of LDH to oxides occurs via a sequence of structural changes with certain impact on the properties of the products. The influence of the prehistory of synthesis on the morphology, cationic distribution and the reactivity of oxygen in the final spinel phases with varying Fe/Co ratios is also evaluated.

Experimental

The iron–cobalt spinel mixed oxides were synthesised by thermal decomposition of pyroaurite-like carbonate hydroxide precursors in dry air flow at temperatures in the range 300—600 °C. The carbonate hydroxides were synthesised as described earlier.[15,16] Thermal analysis of the carbonate hydroxides was performed at a heating rate of 10 K min^{-1} in air, using Al_2O_3 as a reference. The iron and cobalt content in the mixed oxides was determined by X-ray fluorescence analysis. XRD analysis was preformed on a diffractometer with Co $K\alpha$ monochromatized radiation. The IR spectra were taken on a Perkin–Elmer 983 G spectrometer in KBr pellets. Moessbauer spectra were recorded on a spectrometer operating in constant acceleration mode at room temperature and 77 K. The source used was a ^{57}Co/(Cr matrix) and the isomer shifts were referred to α-Fe. The Moessbauer spectra were computer-fitted assuming Lorentzian line shapes, taking into account Debye–Waller correction factors and their temperature dependence. Full-sorption nitrogen isotherms were recorded on a Omnisorp 100 equipment in a continuous flow regime at 77 K. To remove water and other absorbed molecules, before the sorption measurement the samples were pretreated for 2 h at 350 °C in vacuo. Particle dimensions were determined by transmission electron microscopy. Electron spectroscopy for chemical analysis (ESCA) was employed for determining the surface oxygen content on a ESCALAB MkII spectrometer with Mg $K\alpha$ radia-

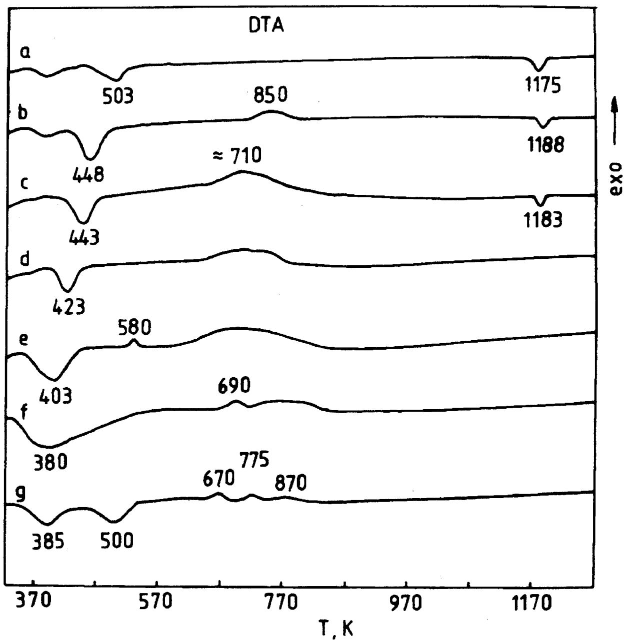

Fig. 1. DTA of layered-type iron–cobalt carbonate hydroxides. a) cobalt carbonate hydroxide, b) Fe/Co = 0.33, c) Fe/Co = 0.5, d) Fe/Co = 1, e) Fe/Co = 2, f) Fe/Co = 3, g) iron carbonate hydroxide.

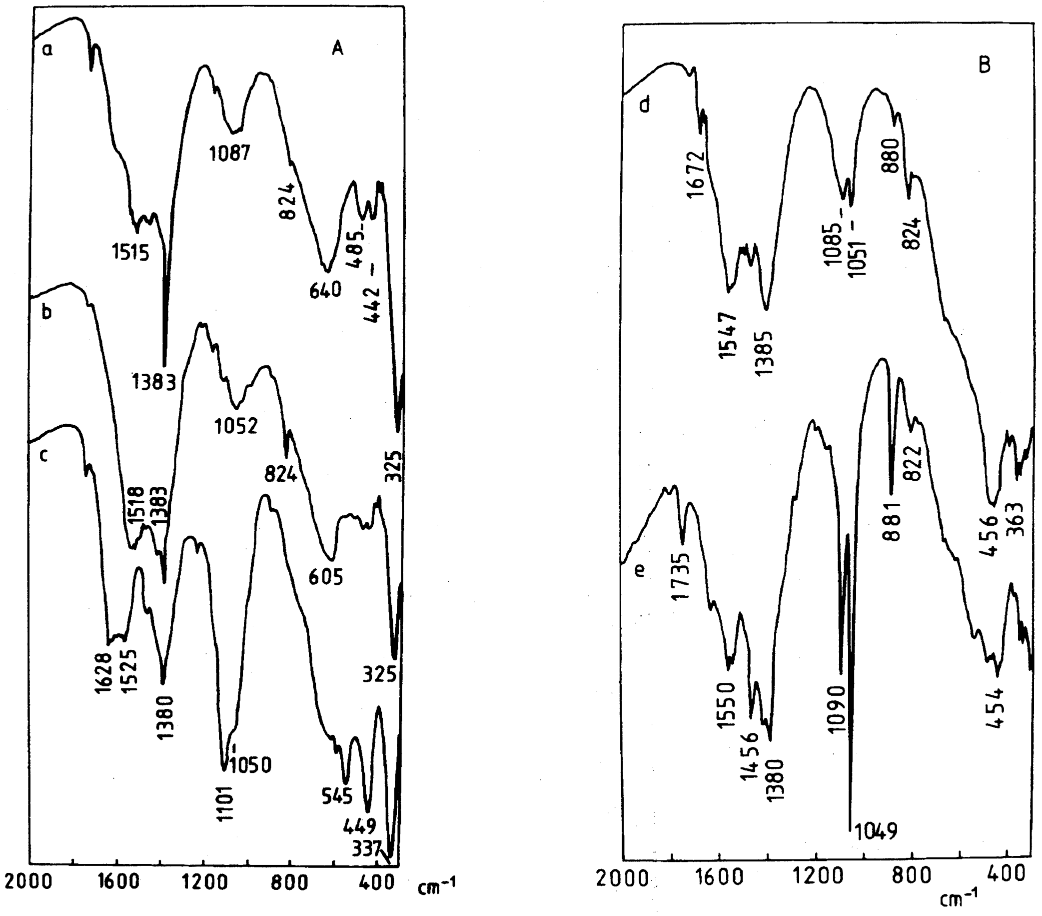

Fig. 2. IR spectra of iron–cobalt carbonate hydroxides in intermediate stages of thermal decomposition (heated to 400 K). a) Fe/Co = 0.33, b) Fe/Co = 0.5, c) Fe/Co = 1, d) Fe/Co = 2, e) Fe/Co = 3.

tion (1253.67 eV). Temperature-programmed reduction in hydrogen (TPR) was performed in a flow system with 5% H_2 in helium at flow rate of 40 ml min^{-1} and heating rate of 20 K min^{-1}. Desorption of non-stoichiometric oxygen was measured under isothermal conditions at different temperatures on a vacuum line with a McLeod manometer.

Results and Discussion

An Infrared Study of the Evolution Process from Layered-Type Carbonate Hydroxides to Spinel Mixed Oxides. Pyroaurite-like carbonate hydroxides are composed from positively charged brucite-like cationic layers of general formula $[\text{M}^{\text{II}}_{1-x}\text{M}^{\text{III}}_{x}(\text{OH})_2]^{x+}$, compensated by anionic interlayers $[\text{CO}_3\cdot n\text{H}_2\text{O}]^{2-}$. Compared to the amorphous carbonate hydroxides of cobalt and iron (Fig. 1 a, g), the thermal transition of crystalline Co–Fe carbonate hydroxides to oxides occurs at lower temperature (Fig. 1b, c, d, e, f). The thermal decomposition of these precursors takes place in one step with simultaneous evolution of carbon dioxide and water in the temperature range 380—450 K. Weakly bound water molecules from the anionic layers are removed below 400 K; that causes the appearance of the first small endothermic peak. The cobalt-rich samples exhibit an endothermic effect above 1150 K due to the transition from a spinel to a rock salt-type structure. Weak exothermic effects are observed at 570—870 K (Fig. 1), related to phase segregation and recrystallization processes as the $\text{Co}_y\text{Fe}_{3-y}\text{O}_4$ compositions with $1.5 \leq y \leq 2.25$ are thermodynamically unstable and segregate to two spinel phases: one rich in cobalt, the other in iron.[2)]

IR spectroscopy is a valuable tool for studying phase transformations at low temperatures. The IR spectra may reveal short range ordering, bond cleavage and bond formation, thus having certain advantages as a complementary method to XRD. The limited periods of treatment in the low-temperature range in most cases do not allow formation of crystalline products and restrict the number of methods to obtain structural information. IR spectra of carbonate hydroxides were recorded at different stages of thermal treatment in air. The coprecipitated layered carbonate hydroxides with different iron/cobalt ratios contain bands characteristic of the vibrations of the free carbonate group (ν_3: 1480—1550 cm^{-1}; ν_1: 1000—1100 cm^{-1}; ν_2: 750—850 cm^{-1}; ν_4: 650—750 cm^{-1}), the bending modes of hydroxyl groups (500—700 cm^{-1}) and the metal-oxygen lattice vibrations (320—400 cm^{-1}).[18—22)] No band can be attributed to the M–OH stretching vibrations; the existence of a broad band at ca. 3400 cm^{-1} indicates that all hydroxyl groups are hydrogen-

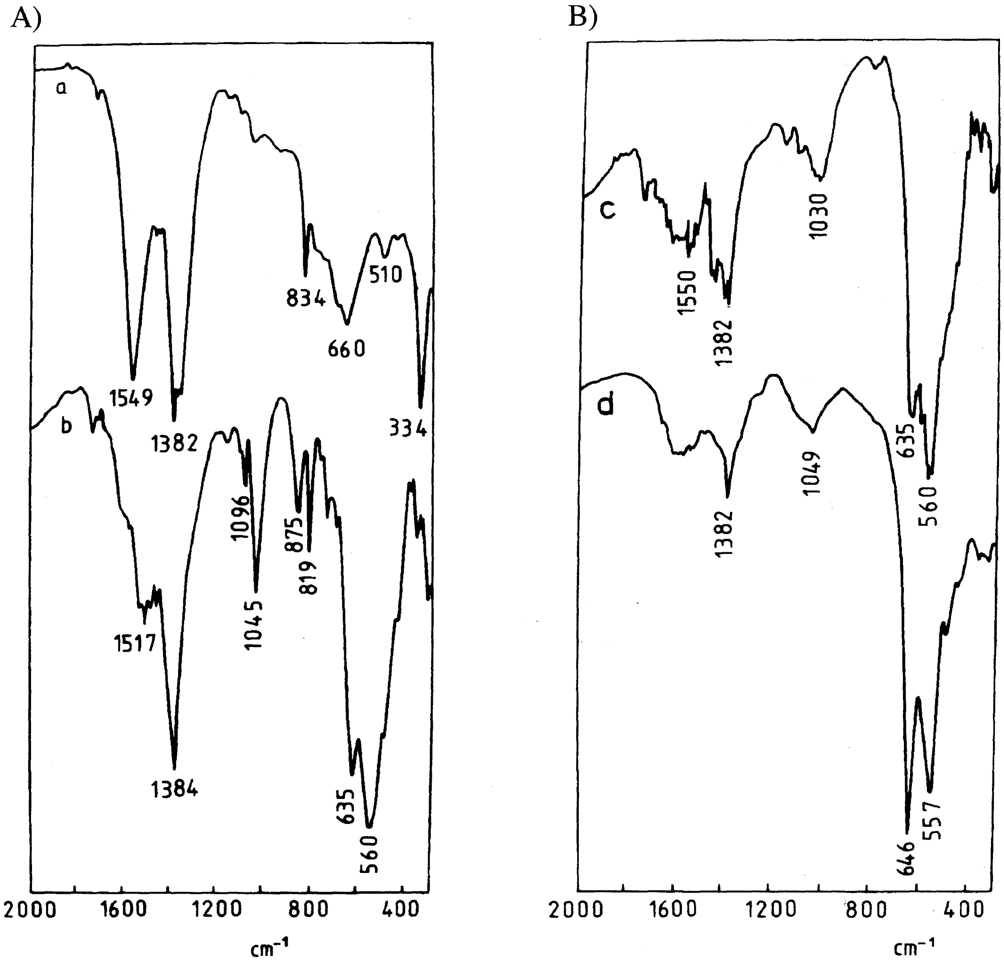

Fig. 3. IR spectra following the evolution of iron–cobalt carbonate hydroxide to iron cobaltite FeCo_2O_4. a) 450 K, b) 480 K, c) 520 K, d) 620 K.

bonded. During thermal decomposition the IR spectra exhibit several band splittings, related to lowering of the symmetry of both the metal cations and the carbonate groups, Fig. 2. Dehydroxylation proceeds simultaneously with carbonate decomposition, evidenced by the single endothermic peak in the DTA. A splitting of the band, originating from the doubly degenerate asymmetric stretching vibration $\nu_3(\mathrm{E}')$ of the carbonate group into two bands with maxima at ca. 1550 and 1380 cm^{-1} is observed. The splitting $\Delta\nu_3$ is related to lowering of the carbonate group symmetry[18,19] from D_{3h} to C_{2v} or C_s and may be interpreted as a result of partial dehydration of both the cationic and anionic layers, followed by direct coordination of the carbonate groups to the metal cations. The symmetric stretching vibration $\nu_1(\mathrm{A}_1')$ is also activated and gives rise to a band at 1000—1100 cm^{-1}. A splitting of the other doubly degenerate vibration of the carbonate group $\nu_4(\mathrm{E}')$ /the in-plane deformation/, generally observed at 680 cm^{-1} can also be expected,[22] but this splitting is of much smaller value and for carbonate hydroxides the bands are obscured by hydroxyl group bending modes. The IR spectra of the carbonate hydroxides with Fe/Co$\geq$1 show two sharp bands at ca. 820 and 880 cm^{-1} (Fig. 2), that are identified as bending M–O–H vibrations and are characteristic for phases of the hydroxide oxide type.[20,21] The XRD patterns did not reveal the presence of a well-defined intermediate phase; only after thermal treatment of pure iron(III) carbonate hydroxide, α-FeO(OH) phase was formed. The appearance of these two intense bands in the IR spectra of iron–cobalt carbonate hydroxides can be attributed to a dehydrated phase with disordered structure close to that of γ-FeO(OH). No free hydroxyl group vibrations could be detected as in the case of the carbonate hydroxide precursors, due to a strong effect of hydrogen bonding. The process of thermal decomposition was followed also with one sample rich in cobalt, Fig. 3. The spectrum in Fig. 3a displays a clear splitting $\Delta\nu_3$(bands at 1549 and 1382 cm^{-1}) and smaller splitting effect $\Delta\nu_4$ (band at 660 cm^{-1} with shoulder at ca. 685 cm^{-1}). Further thermal treatment causes appearance of the two sharp bands at 819 and 875 cm^{-1} indicating hydroxide oxide intermediates and an intense band at 560 cm^{-1} along with a weaker band at 635 cm^{-1}— the last two corresponding to a spinel cobaltite phase. Our results are in accordance with the mechanism of hydrotalcite thermal decomposition, proposed in Ref. 12, where the formation of 3-dimensional structure from a layered one proceeds via an intermediate, partly dehydroxylated structure, where a large part of the cations are still in octahedral coordination.

Spinel ferrites and cobaltites belong to the $Fd3m$ space

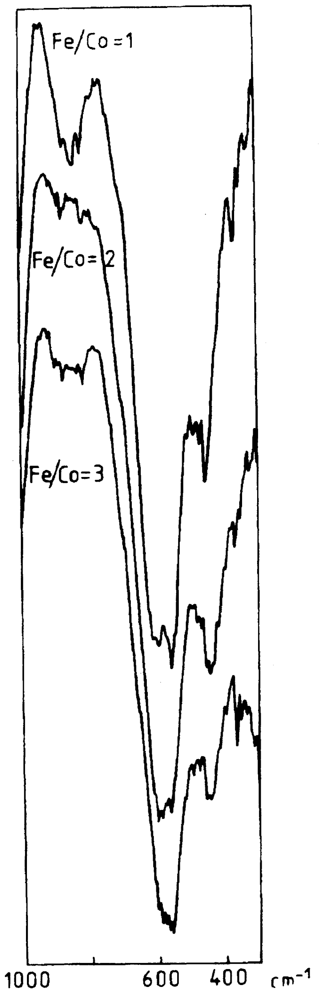

Fig. 4. IR spectra of iron–cobalt mixed oxides, synthesised at 620 K.

Table 1. Oxygen Desorption at Different Temperatures for Iron–Cobalt Spinel Oxides, Synthesised at 300 °C, Compared to the Surface Oxygen Content

	Oxygen desorbed, (cc g^{-1})		
Temperature/ °C	Fe/Co = 0.5	Fe/Co = 1	Fe/Co = 2
400	0.1	0.8	0.4
450	0.3	1.4	1.0
500	0.4	2.0	2.5
550	0.8	3.5	3.8
600	1.0	5.2	5.4
650	1.7	6.5	6.0
700	2.3	7.0	6.0
	Oxygen to metal cation (Fe+Co) surface atomic ratio /ESCA/		
	2.26	2.18	3.0

group and possess four IR active vibration modes.[20,23] The two higher frequency bands are assigned to A–O–B_3 and B–O–B_2 stretching vibrations in the spinel lattice (A stands for cations in tetrahedral coordination, B — for the octahedral ones). Although the main contribution to both vibrational modes belongs to the octahedrally coordinated cations, the domination of the 560 cm^{-1} band indicates a phase with still prevailing octahedral symmetry of the cation coordination, inherited from the precursor compound (Figs. 3 and 4). The diffusivity of cations from the cationic layers is strongly restricted and only at the final stage of crystallisation do these two bands reach comparable intensities, thus proving the slower process of occupation of the tetrahedral sites. The other two bands of lower frequency and intensity are interpreted as due to vibrations of tetrahedral and octahedral cations relative to each other.[20)]

For iron rich spinels, the main bands are shifted to lower frequencies, indicating weaker force constants Fe–O, compared to Co–O. In the IR spectra of mixed oxide samples with Fe/Co$\geq$1, synthesised at temperatures below 650 K,

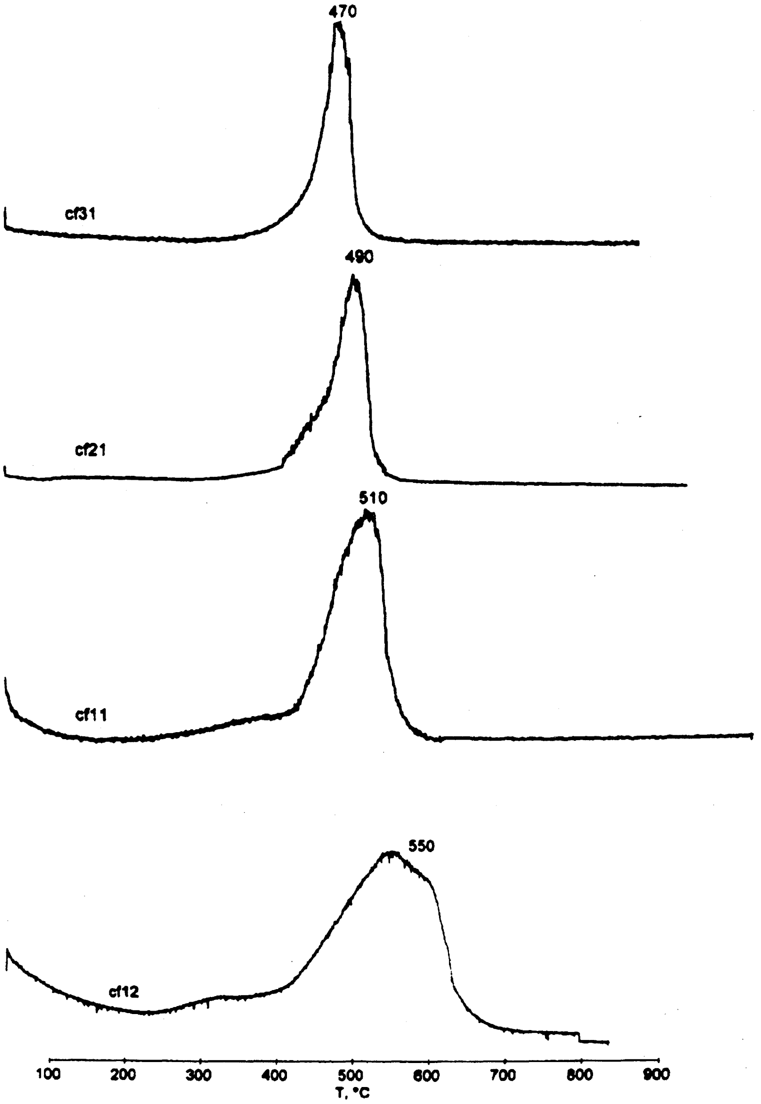

Fig. 5. TPR spectra of cobalt–iron mixed oxides.

Table 2. Pore Distribution and Specific Surface Areas of Iron–Cobalt Mixed Oxides

Sample Fe/Co ratio	BET surface area	Total pore volume (cc g^{-1})	Pore volume (cc g^{-1}) at radii		
	$m^2\,g^{-1}$	(r > 10 Å)	50–100 Å	100–200 Å	200–300 Å
Fe/Co = 0.5	67	0.18	0.02	0.03	0.04
Fe/Co = 1.0	116	0.58	0.09	0.20	0.10
Fe/Co = 2.0	102	0.56	0.15	0.22	0.05

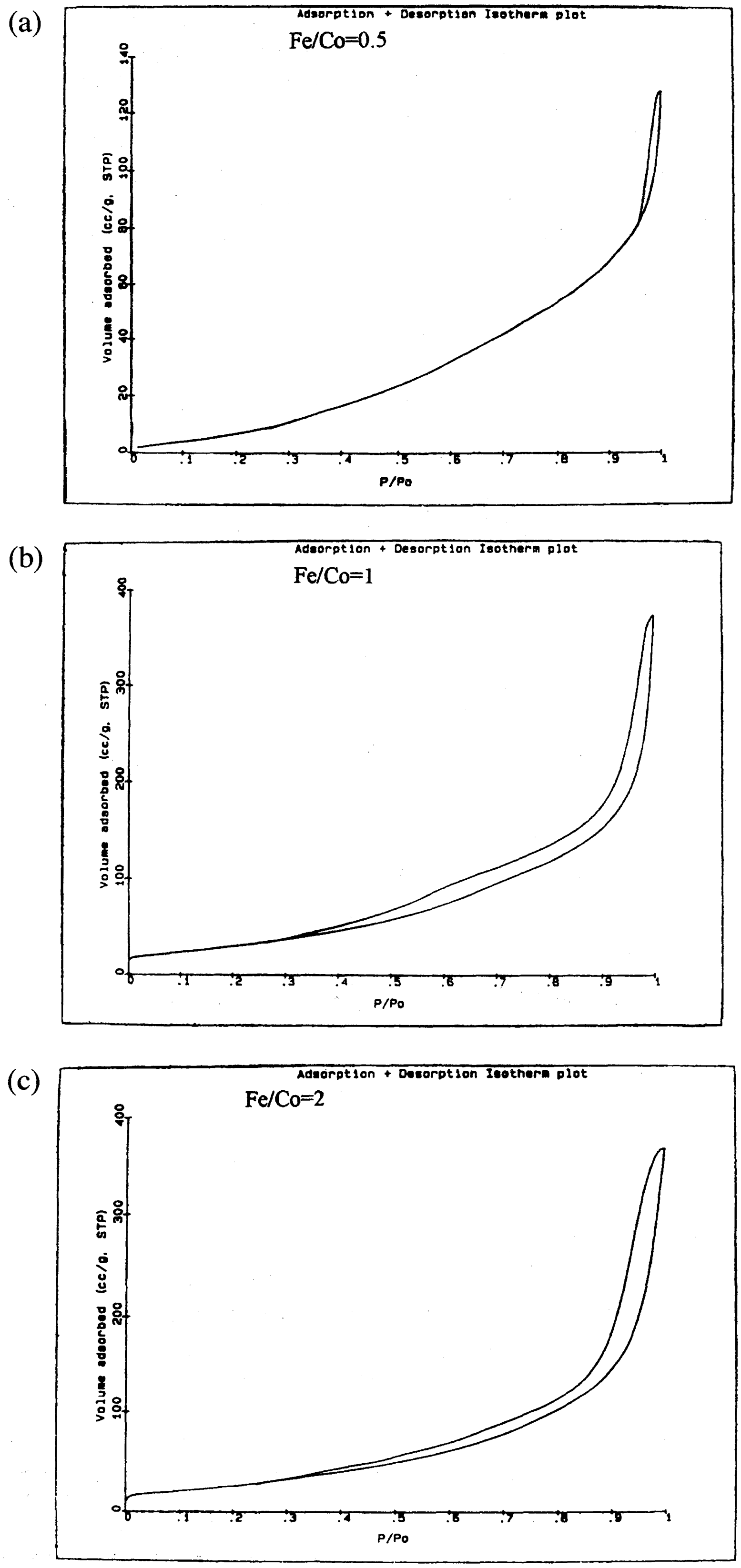

Fig. 6. Full-sorption nitrogen isotherms of iron–cobalt mixed oxides.

broad bands with fine structure (Fig. 4), typical of the γ-iron oxides containing cation vacancies are present.[24] The existence of ordered cationic vacancies in octahedral positions of spinel may give rise to 21 additional bands in the IR spectrum.[25] The vacancies in this case form no superstructure, because the particle size is too small, and no additional lines are registered in the XRD patterns. The IR band at 630 cm^{-1} is characteristic of these spinels, possessing octahedral vacancies with a certain degree of ordering.[9,24] At 870 K the fine structure of the IR spectrum of cobalt ferrite almost disappears and only the two strong bands of approximately equal intensity at 388 and 592 cm^{-1} remain. Above that temperature, the presence of cationic vacancies in the spinel lattice may be excluded.

A Study of the Oxygen Reactivity by Temperature-Programmed Reduction and Oxygen Desorption. The desorption of non-stoichiometric oxygen was performed in isothermal conditions at different temperatures, Table 1. Desorption from the mixed oxides with higher iron content (Fe/Co = 1 and Fe/Co = 2) is more intensive. The sample with ratio Fe/Co = 1 desorbs the largest amount of oxygen, although the surface oxygen-to-metal ratio is lowest. It should be kept in mind, however, that both spinel oxides with ratios Fe/Co = 0.5 and Fe/Co = 1 undergo phase segregation at temperatures above 500 °C to two spinel phases of different iron/cobalt ratios. The cobalt ferrite sample (Fe/Co = 2) is stable in the whole temperature range and desorbs oxygen most intensively in the range 500—600 °C. The excess surface oxygen is quite high, compared to the stoichiometric value of 4/3, in agreement with previous studies on cation-deficient ferrites.[15,16] The TPR spectra (Fig. 5) of the spinel mixed oxides show a single peak with maximum position, depending on the iron/cobalt ratio. A broadening is observed for the iron-rich samples and a shift of the peak maxima towards higher temperatures. Cobalt ferrite is reduced in the range 400—650 °C with peak maximum at 550 °C and a shoulder at ca. 600 °C. Elementary steps of Fe^{3+}, Co^{3+}, and Co^{2+} reduction cannot be distinguished in the TPR spectra, leading to the suggestion that the more easily reducible cations (in this case Co^{3+} and Co^{2+}) promote the reduction of iron cations. A similar effect is known for oxides containing copper or silver cations and is explained by the high rate of metal cluster formation. These clusters are able to participate further in the reduction as active centers.[26]

Morphology and Pore Distribution Study. The thermal decomposition of precursors with different iron/cobalt ratios yield mixed oxides with high specific surface areas, Table 2. The powders are polydisperse, composed from particles of mostly spherical shape with dimensions in the range 3—12 nm, determined by TEM. The full-sorption nitrogen isotherms of spinel oxide samples with atomic ratios Fe/Co = 0.5, Fe/Co = 1, and Fe/Co = 2 are of type IV according to the BDDT classification,[27] typical of mesoporous materials (Fig. 6). Significant hysteresis is observed for iron-rich compositions Fe/Co = 1 and Fe/Co = 2, suggesting the existence of ink-bottle pores. The major contribution to pore volume comes from pores with radii 100—300 Å.

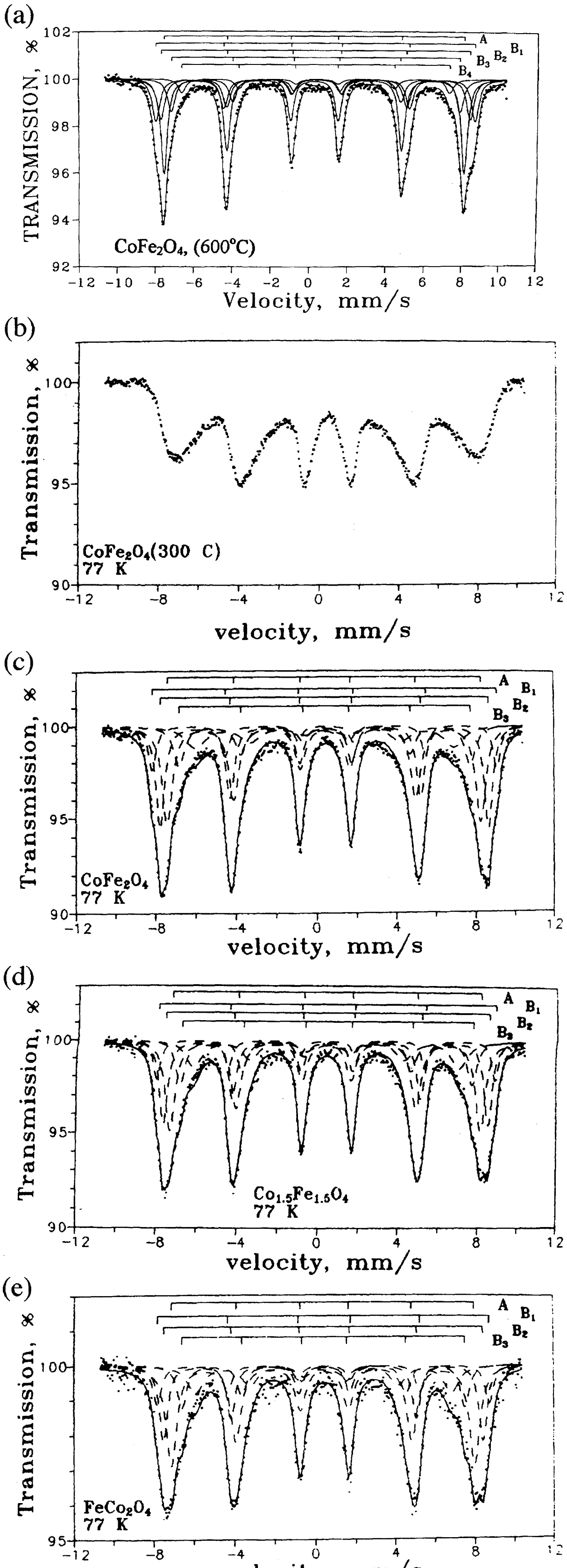

Fig. 7. Moessbauer spectra of iron–cobalt mixed oxides. The temperature of synthesis is noted in brackets. The temperature of recording of the spectra is also pointed /RT : room temperature/.

Table 3. Moessbauer Parameters and Iron Cation Distribution of Iron–Cobalt Mixed Oxides, Obtained by Thermal Decomposition of the Corresponding Iron–Cobalt Carbonate Hydroxides

Sample composition	Synthesis temperature	Isomeric shift/mm s^{-1}		Internal magnetic field H_{eff} [kOe]					Fe(III) distribution, at %	
	T/°C	δ(1A)	δ(2–5B)	A	2B	3B	4B	5B	Tetra	Octa
$CoFe_2O_4$	600	0.274±0.007	0.371±0.008	486	516	500	466	433	40±3	60±3
$CoFe_2O_4$	400	0.41 ±0.01	0.44 ±0.01	497	526	497	459	415	36±3	64±3
$Co_{1.5}Fe_{1.5}O_4$	300	0.42 ±0.01	0.44 ±0.01	480	523	502	451	410	37±4	63±4
$FeCo_2O_4$	300	0.43 ±0.01	0.44 ±0.01	469	513	494	437	395	41±5	59±5

Moessbauer Characterization of the Mixed Oxides. Cobalt(II) has stronger preference for octahedral coordination than Fe(III), according to the crystal field stabilization energies,[28] but not enough to reach complete inversion of the spinel, as in $NiFe_2O_4$.[16] A partly inverse spinel distribution in a broad temperature and compositional range may be expected. Inclusion of cobalt(II) in both tetrahedral and octahedral positions of the spinel structure of ferrites results in line broadening of the Moessbauer spectrum. The distribution of iron cations among octahedral and tetrahedral sites, evaluated from the component areas of the spectrum (Fig. 7), permit one to write the cation distribution of cobalt ferrite, synthesised at 600 °C as $[Co_{0.2}Fe_{0.8}]_{\mathrm{tetra}}[Co_{0.8}Fe_{1.2}]_{\mathrm{octa}}O_4$. The unit cell parameter for this sample, determined from the XRD data, is $a = 8.349 \pm 0.003$ Å. The presence of cation vacancies may be neglected above 600 °C. According to Sawatzky et al.,[29] the Moessbauer spectrum deconvolution model regards five types of iron(III) coordination—tetrahedral (A) and octahedral with 0, 1, 2, and 3 nearest cobalt(II) neighbors (B_1, B_2, B_3, and B_4), placed on the six nearest cationic sites. The room temperature (RT) Moessbauer spectra of all spinel samples synthesised below 400 °C contained a central doublet, due to small particle superparamagnetism. It could be resolved at a recording temperature of 77 K. Two samples of cobalt ferrite, synthesised at 300 and 400 °C, are compared (Fig. 7). The sample synthesised at 300 °C gives rise to a rather broad Moessbauer spectrum, leading us to the conclusion that not only is the particle size small, but the framework contains many imperfections. A sintering temperature of 400 °C allows detection of a well-resolved spectrum for $CoFe_2O_4$, while 300 °C is a sufficiently high temperature for the crystallisation of cobalt rich samples $FeCo_2O_4$ and $Co_{1.5}Fe_{1.5}O_4$. The Moessbauer parameters and cation distributions are shown in Table 3. The relative proportion of Fe(III) cations on tetrahedral and octahedral sites does not change significantly with the iron/cobalt ratio and no temperature dependence was determined in the range 300—600 °C. The spinel phases, obtained at low temperatures have very close values for the isomeric shifts of cations in octahedral and tetrahedral sites (Fig. 7 and Table 3), in agreement with the suggestion for cation deficiency and a thermal decomposition mechanism passing through an intermediate of randomly oriented octahedral cations.

Conclusion

The use of layered-structure carbonate hydroxide precursors of pyroaurite type in the synthesis of iron–cobalt mixed oxides yields partly inverse spinel phases of high despersity and porosity via hydroxide oxide-type intermediates. The samples with higher iron/cobalt ratios, synthesised at 300 °C contain a high vacancy concentration, but as the particle size is small, vacancy ordering is not detected. Non-stoichiometry is related to high oxygen reactivity, as determined by TPR.

References

1) T. Takada, "Ferrites: Proceedings of the ICF3 September–October 1980," ed by H. Watanabe, Sh. Iida, and M. Sugimoto, Center for Acad. Publications, Tokyo.

2) A. Pelton, H. Schmalzried, and J. Sticher, *Ber. Bunsenges. Phys. Chem.*, **83**, 241 (1979).

3) W. Cares and J. Hightower, *J. Catal.*, **23**, 193 (1971).

4) F. Cavani, F. Trifiro, and A. Vaccari, *Catal. Today*, **11**, 173 (1991).

5) A. Tseung and J. Goldstein, *J. Mater. Sci.*, **7**, 1383 (1972).

6) H. Tamura and E. Matijevic, *J. Colloid Int. Sci.*, **90**, 100 (1982).

7) J. L. Martin de Vidales, O. Garcia-Martinez, E. Vila, R. Rojas, and M. Torralvo, *Mat. Res. Bull.*, **28**, 1135 (1993).

8) B. Gillot, F. Jemmali, and A. Rousset, *J. Solid State Chem.*, **50**, 138 (1983).

9) J. Jimenez-Mateos, J. Morales, and J. Tirado, *Reactiv. Solids*, **7**, 235 (1989).

10) R. Allmann, *Chimia*, **24**, 99 (1970).

11) M. Bellotto, B. Rebours, O. Clause, J. Lynch, D. Bazin, and E. Elkaim, *J. Phys. Chem.*, **100**, 8527 (1996).

12) M. Bellotto, B. Rebours, O. Clause, J. Lynch, D. Bazin, and E. Elkaim, *J. Phys. Chem.*, **100**, 8535 (1996).

13) S. Miyata, *Clays Clay Miner.*, **23**, 369 (1975).

14) H. Hansen and C. Koch, *Appl. Clay Sci.*, **10**, 5 (1995).

15) E. L. Uzunova, D. Klissurski, I. Mitov, and P. K. Stefanov, *Chem. Mater.*, **5**, 576 (1993).

16) E. L. Uzunova, D. Klissurski, and S. Kassabov, *J. Mater. Chem.*, **4**, 153 (1994).

17) H. Hansen and C. Koch, *Inorg. Chem.*, **33**, 5363 (1994).

18) K. Nakamoto, "Infrared and Raman Spectroscopy of Inorganic and Coordination Compounds," Wiley & Sons, New York (1978), pp. 283 and 380.

19) G. Busca and V. Lorenzelli, *Mater. Chem.*, **7**, 89 (1982).

20) V. Farmer, "Infrared Spectra of Minerals," Mineralogic Soc., London (1974).

21) G. Busca, G. Ramis, M. Prieto, and V. Escribano, *J. Mater. Chem.*, **3**, 655 (1993).

22) H. Britzinger and R. Hester, *Inorg. Chem.*, **5**, 980 (1966).

23) M. Ishii, M. Nakahira, and T. Yamanaka, *Solid State Commun.*, **11**, 209 (1972).

24) B. Gillot and F. Bouton, *J. Solid State Chem.*, **32**, 303 (1980).

25) W. White and B. De Angelis, *Spectrochim. Acta, Part A*, **23**, 985 (1967).

26) R. Anderson, in "Catalysis, Vol.4, Hydrocarbon Synthesis, Hydrogenation and Cyclization," ed by P. Emmett, Reinhold Publ. Co., New York (1956), p. 82.

27) S. Gregg and K. Sing, "Adsorption, Surface Area and Porosity," 2nd ed, Academic Press, New York (1982).

28) A. Wells, "Structural Inorganic Chemistry," 5th ed, Clarendon Press, Oxford (1986), Chap.13.

29) G. Sawatsky, F. Van der Woude, and A. Morrish, *Phys. Rev.*, **187**, 747 (1969).